Journal of Engineering and Applied Sciences 12 (17): 4475-4481, 2017
ISSN: 1816-949X

Design and Simulation of MEMS Type Cathodic Ray Generator

Sadegh Mohammad Zadeh Bazarchi and Ebrahim Abaspoor Sani
Faculty of Electrical Engineering, University of Urmia, Urmia, Iran

Abstract: In this study is about the design and simulation of Hot Cathode Filament (HCF) for genesis of Cathode Ray (CR) at the MEMS scale. On the plan of this study nickel with a layer of oxide forms the cathode and is capable of emitting electrons with 50 nA current at the temperature of 750°C. Also, it is considered that the temperature is almost constant along the cathode and the emission of electrons is uniform in different parts. Furthermore, the cathode temperature is independent of the vacuum pressure. The grid voltage which provides the initial energy for electros is controllable providing the ability of turning the beam ON and OFF. It must be mentioned that the power consumption of the cathode is low (69.2 mW) and its dimensions are 2.5×1.5×0.5 mm. For the case of no target utilization, the energy of electrons reaches the value of 429 eV. On the design of this scheme the MEMS technology has been employed and the distance of anode network, height, thickness, number of the rods and other specifications of the anode to achieve the highest number and highest energy for the electrons have been determined by simulations carried out using COMSOL. In addition, the analysis of cathode temperature, cathode tension, electron movements, potential and electric field have been performed in this study.

Key words: MEMS type ionization gauge, MEMS type vacuum sensor, MEMS type cathode ray, vacuum pressure sensor, micro heater, MEMS type X-ray supply

INTRODUCTION

This plan already exists and can be used in MEMS type micro pump, MEMS type X-ray production system, MEMS type CR imaging and MEMS type ionization vacuum gauge. This system operates at low vacuum and emits the electrons by means of hot cathode. The released electron beam can ionize the environment gas atoms as a result of collision with them and generate positive ions along with secondary electrons. Then, the positive ions and secondary electrons will be accumulated by collector and the anode, respectively. As the process continues, the gas atoms will be reduced and the environment tends to behave like a high level vacuum and as a result, we will have an electric vacuum pump. This system with hot cathode, the anode network and the collector can be considered as a vacuum sensor (Note, 2017). It is because the accumulated ions at the collector wire produce a current denoted by I_c which is directly proportional to the existing number of atoms at the vacuum environment and in other words the vacuum pressure determines the flowing current across the collector wire. This system is best known as hot-filament ionization vacuum gauge or Bayard-Alpert hot-filament gauge.

The CR is used to produce the X-ray where the beam has an energy varies from 100-100 keV. Two well known classes of the beam are soft and deep ones and because of no transition losses at the space in addition of medical industrial and crystallography applications it is widely used in space communications and satellite contacts (Li and Mou, 2016). One of the main attempts in this criterion is to achieve the miniaturization with the goal of reducing thermal dissipations on the hot cathode along with increment of ON/OFF frequency for the grid (Li and Mou, 2016). CR imaging (Spallas *et al*., 2016) is another application in which this plan can be involved in.

The cold ionization cathode has been previously used for construction a MEMS type micro pump (Grzebyk *et al*., 2015), therefore, the proposed scheme which provides the CR at the MEMS dimensions and employs hot cathode can also be utilized for micro pump design.

On the hot cathode section, the gas pressure of environment cools down the cathode and as a result, the need for a temperature sensor and a current controller is inevitable. But in this study, a procedure has been used in which there is no dependency between temperature and pressure of vacuum environment. This method can also be employed for MEMS type gas sensor heaters where the environment pressure variations don't have any effect on the performance of the sensor (Joy and Antony, 2015).

Corresponding Author: Sadegh Mohammad Zadeh Bazarchi, Faculty of Electrical Engineering, University of Urmia, Urmia, Iran

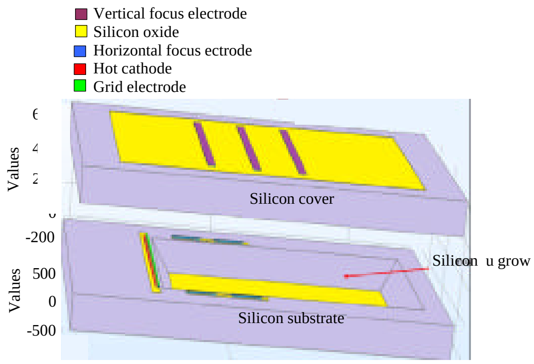

Fig. 1: General scheme of MEMS type CR production system

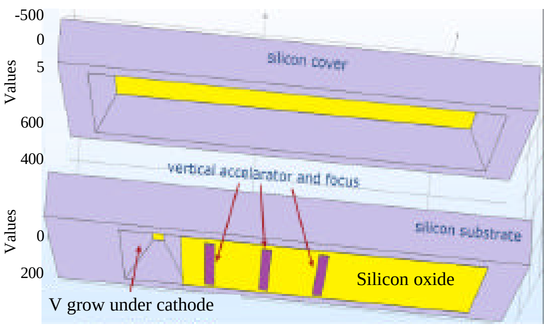

Fig. 2: Lower view of the general scheme of MEMS type CR production system

In this research, Nickel with Alkali metal oxide overlay has been used for hot cathode which reduces the work function and enables the cathode to emit electrons at the temperature of 850°C. Low operating temperature considerably affects the efficiency and power consumption of the system.

General plan: Figure 1 and 2 show the general design scheme from upper view in which the cathode and grid are visible but more details will be provided later. As shown in Fig. 1 the scheme is composed of a silicon base and a cover where these two parts will be bonded in vacuum environment. At the base and by means of anisotropic acidized etching, a pit has been created while the same thing has been carried out for the silicon coverage. The upper and lower pits together, provide a space for focusing and movement of CR. According to Fig. 1 at the beginning of the pit in silicon base the cathode and grid network have been located in which the CR is produced and accelerated. In addition of the acceleration, the grid network has the responsibility for switching of the CR to ON/OFF. On the sides of the lower silicon pit, the horizontal focusers are located and with the help of repulsion force originating from their negative bias voltage, they concentrate the CR in the middle of the tip. The vertical focusers and accelerators are positioned under the tip over the oxide layer and some of them accelerate the CR using positive voltage while the others have the role of focusing by means of negative voltage.

Figure 2 shows the general plan from lower view in which a tip has exactly been constructed under the hot cathode. Doing this, the thin oxide layer under hot cathode prevents any heat exchanges (more details will be discussed in study).

MATERIALS AND METHODS

Hot cathode part: The undertaken considerations on the design of MEMS type hot-filament cathode gauge are as follow:

- The cathode filament layer must be implementable by MEMS technology with the least mechanical issues
- The filament must be capable of generating the temperature of 750°C with the lowest power and the temperature should be constant over the rod
- The heat transfer to the silicon sub layer should be as minimum as possible while the heat convection to the environmental gas must be negligible so that the vacuum pressure variations won't affect it
- The electron emission level must be suitable

In this design, a layer of Nickel with MEMS technology and by means of electroplate procedure over silicon oxide layer is employed. With alkali metal oxide layer deposition over Nickel its work function will be considerably decreased where it can emit electrons at the temperature of 750°C. In Fig. 3, the details for cathode filament are shown.

According to Fig. 3, the cathode filament is located over a thin layer of silicon oxide while the under layer is etched in anisotropic form so that the heat transfer between filament and silicon framework will be reduced and the effects of environmental gas pressure variations can be eliminated. In Fig. 4, it is clear that the cathode layer is attached to the anchor and is composed of two A and B parts in which A is thin and B is thick to keep the temperature constant along the cathode layer.

Equation 1 denotes the Richardson-Dutchman theorem for thermal emission in the cathode filament in which T refers to the temperature in Kelvin, k_B denotes the Boltzmann Constant and φ introduces the work function of filament in electron volts (Go, 2012).

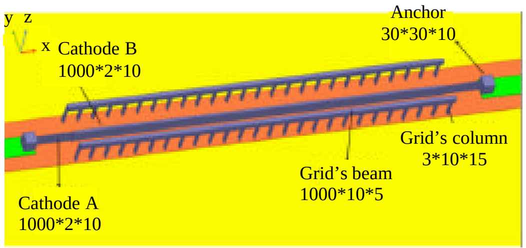

Fig. 3: The details for cathode and grid design

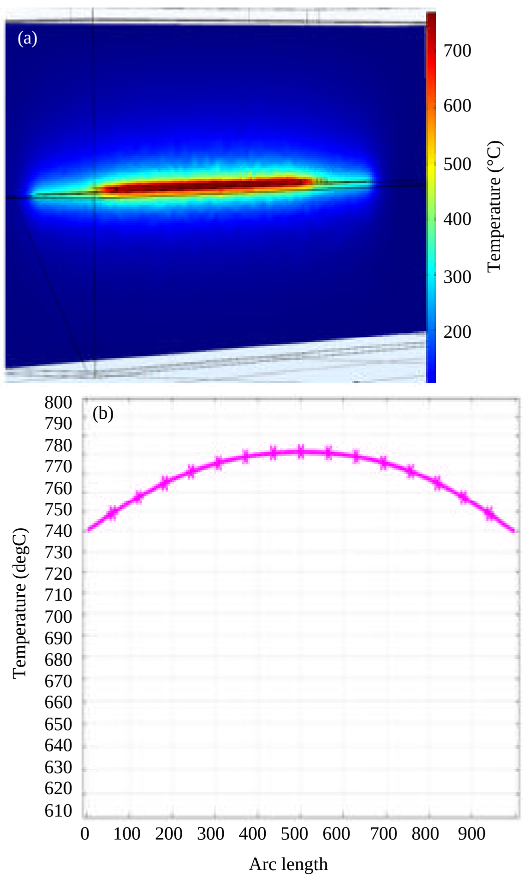

Fig. 4: a) COMSOL simulation over the length of cathode and b) the curvature of temperature changes over cathode length

$$J = 1.20173\times10^{6}\times\exp\left(-\frac{\varphi}{k_B T}\right) \quad (1)$$

The work function for Nickel wit oxide layer is equal to 1.1 eV. As a result, the current density in 750°C becomes 5 A/m^2. The dimensions of cathode filament wire depend on the design considerations and different parameters as follows: the current value, cathode wire current density of J = 5 A/m^2, constant temperature of 750°C provision along the cathode wire the independency of cathode temperature to the gas pressure, low power dissipation and compatibility with MEMS technology. Table 1 briefly illustrates the physical dimensions in optimum conditions using COMSOL5 Software. For example, the dimensions of main part of the cathode are designed in a way so that the electron emission current could be obtained:

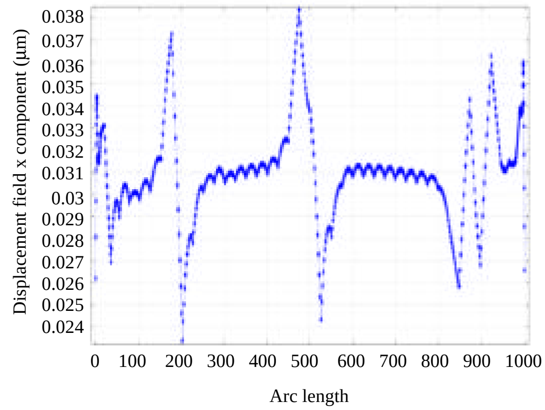

Fig. 5: Simulation of mechanical relocation analysis of the cathode under the effect of temperature using COMSOL

Table 1: Details and dimensions of the cathode

Factor	Cathode main section (B)	Cathode secion (A)	Anchor	Pad	Oxide layer
Material	Oxide coated nickel	Nickel	Nickel	Al	Sio_2
Length	1000	100	30	300	2200
Width	6	5	30	50	80
Thiknes	10	10	10	1	1

$$I_{emission} = J\times1000\times10\ \mu m = 0.05\ \mu A \quad (2)$$

Considering the power dissipation of 69.2 mW for each filament of the cathode the operating temperature of 750°C can be obtained. The temperature has its maximum value in the center but because both sides of the cathode are attached to anchor and pad, the temperature will considerably drop at both terminals of the filament. Hence, the side parts of the filament in part A are chosen thinner to increase the electrical resistivity which compensates the thermal drop. Using this method, thermal distribution of the cathode over main part B remains constant and the COMSOL simulation results illustrated in Fig. 5, justify it. Figure 4 shows the simulation results for mechanical tension analysis of the cathode under the effect of temperature. The maximum changes of cathode height denoted as 0.038 µm is specified in Fig. 4 which constitutes 0.38% of total height. As a result, no changes happen for the electron emission angle and its focus. In this scheme, the cathode filament is not hanging in the air and is located over silicon oxide layer of the base. But from the above parts and by means of vacuum environment gas, there exists a thermal exchange and if the ratio of exchange is more than the normal value, it will decrease the temperature of cathode which reduces electron emission ratio and necessities the use of current controller to consolidate the temperature. In this study, oxygen is considered as the vacuum gas and for different degrees of vacuum the cathode temperature has been simulated.

Equation 2 shows thermal conductivity coefficient changes as a function of pressure and its temperature (Lasance, 2002):

$$k = \frac{k_0}{\left(1 + \frac{7.6\times10^{-5}\times T}{p\times d}\right)} \quad (3)$$

Where:

- k_0 = The conductivity coefficient for room temperature and atmospheric pressure
- T = The gas temperature
- p = Implies on gas pressure
- d = The height distance of the gas

Figure 6 shows thermal conductivity characteristics of the hottest point of the cathode versus the vacuum pressure changes which demonstrates that the cathode temperature is constant for vacuum pressures under 10^{-3} torr.

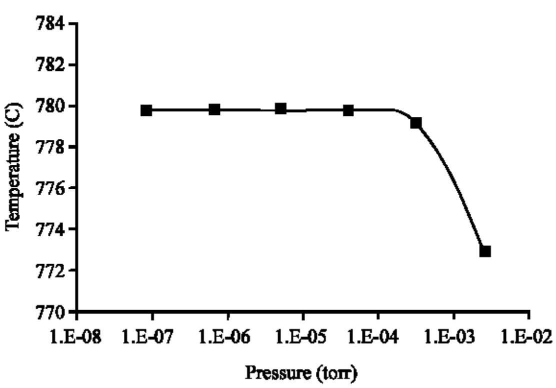

Fig. 6: Cathode temperature changes versus vacuum pressure variations

RESULTS AND DISCUSSION

The accelerator, focuser and grid: The details for grid electrode are shown in Fig. 3. The grid network is composed of a number of metal column rods along with one horizontal rod. The material and design method is the same as the process of cathode implementation. The grid characteristics and its distance with cathode in order to establish the electric field and the electrostatic attraction for the electrons are very important parameters in definition of initial acceleration and initial focus of the CR. Therefore, the Charged Particle Tracing (CPT) simulation in COMSOL for emulation of best conditions is being utilized. Table 2 illustrates the specifications for grid, accelerator and focuser.

In Fig. 7 and 8, the electric potential of the plan for XZ and XY cross sections have been demonstrated. It must be noted that the applied potentials to accelerators and focusers are for concentration of the CR while enough energy must be provided for these parts. Electrons with high energy value will travel with high speeds and this factor makes them harder to be focused. Hence, the third electrode for the accelerator is used to solve this problem. In Fig. 9, the electric field in different parts of XZ cross section by means of arrows is illustrated and corresponding electric fields of the focuser and accelerator have completely been specified.

For electron beam analysis again the CPT simulation of COMSOL is used. The meshing of cathode must be in a way so that the electrons can be distributed uniformly. For the simulation of Fig. 10, the movements of 320 electrons distributed over the cathode and their motions in the direction of accelerator and focuser can be observed. Also in Fig. 11 by applying -10 V to the grid, the emission is completely stopped. Therefore, an electric pulse with the amplitudes of +100 and -10 V can start and stop the emission process. The energy of electrons at the moment of reaching the target is also important. As the goal of this research is to produce and concentrate the CR y mean of MEMS technology, the target is not employed for X-ray beam. For the case of target utilization and by applying a big positive value of electric potential to the target, the energy of electrons can reach to several keV. In Fig. 12, the energy of electrons for different times are shown. By means of simulation results obtained from

Table 2: Material type and the dimensions for grid and collector (to μm)

Factors	Material	No.	Lenght	Width	Heigh	Distance to cathode	Vertical distance to center	Horizintal distance to center
Grid columns	Ni	26	10	3	15	20	0	0
Grid upper pencil	Ni	1	10	1000	5	20	0	0
Grid lower layer	Ni	1	10	1000	1	20	0	0
Vertical accelerators	Al	6	50	1000	1	-	+200-200	0
Horizontal focuss and focuss	Ni	4	200	10	10	-	0	+500-500

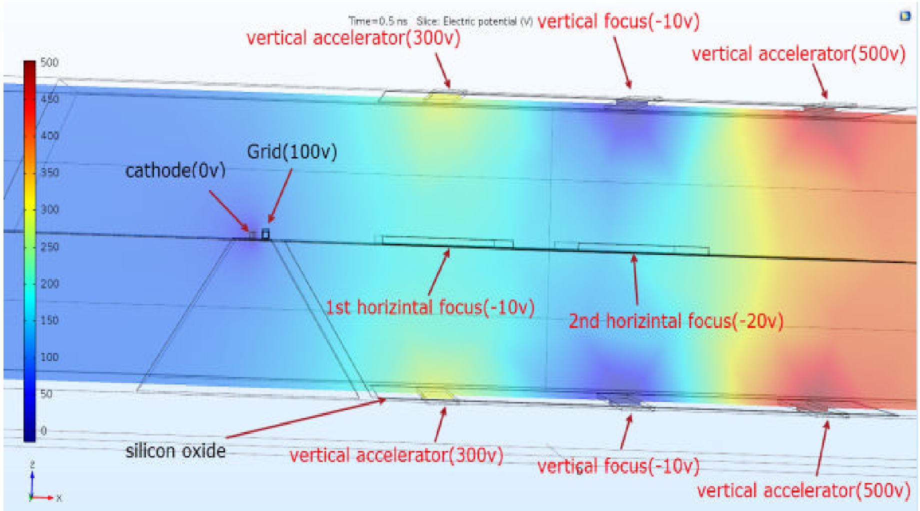

Fig. 7: The electric potential for XZ cross section

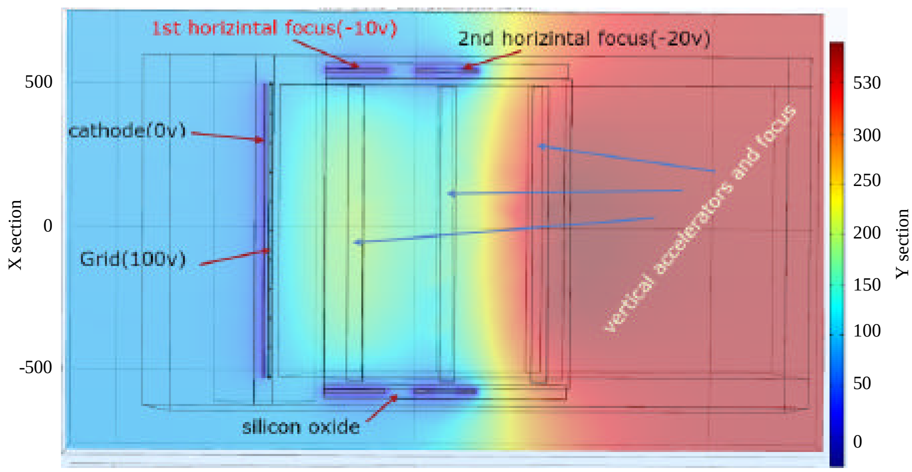

Fig. 8: The electric potential for XY cross section

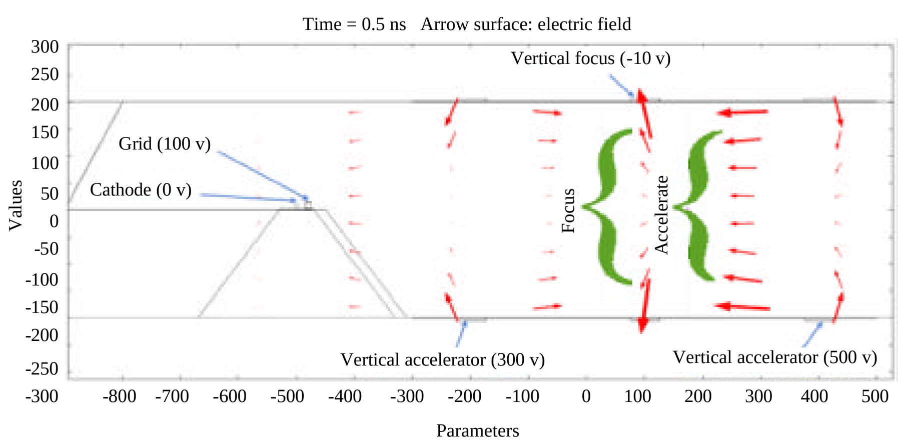

Fig. 9: The electric field direction using arrows for XZ cross section

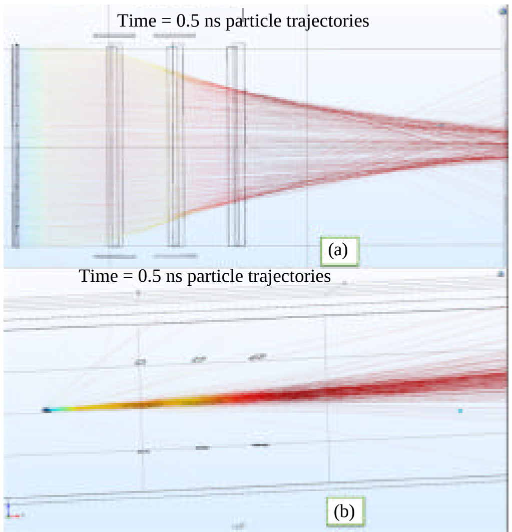

Fig. 10: Motion path for the electrons with grid voltage of 100V: a) Upper view and b) Lower view

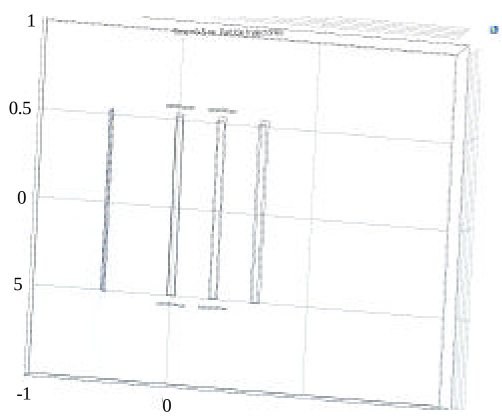

Fig. 11: CR OFF state for grid voltage of -10 V

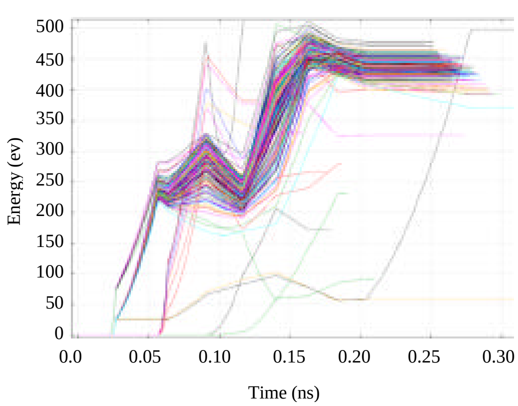

Fig. 12: The energy of electrons according to time changes

CPT, the collision time of the electrons to the target is almost 0.27 ns. With the help of MATLAB and by averaging the energy at 0.27 ns the average energy can be obtained which demonstrates the value of 429 eV.

CONCLUSION

In this study, a new method for production of CR using MEMS technology has been proposed which can be widely used in different applications ranging from X-ray generation for space communications to MEMS type hot-filament ionization vacuum sensor. Some other applications like MEMS type micro pump and CR imaging can also be concluded among the advantages of proposed scheme.

In the plan of this research the operating temperature is very low (750°C) while the power consumption is 69.2 mW and because of the used procedure, the cathode temperature is independent of vacuum pressure. Its small volume (2.5×1.5×0.5 mm) provides the integration feature alongside the other systems. By applying the electric pulse with the amplitudes of +100 and -10 V to the grid, the CR beam with the energy of 429 eV can easily be turned on and off while its response time is almost 0.27 ns.

REFERENCES

Go, D.B., 2012. Gaseous Ionization and Ion Transport: An Introduction to Gas Discharges. University of Notre Dame, Notre Dame indiana, Pages: 71.

Grzebyk, T., A. Gorecka-Drzazga, J.A. Dziuban, K. Maamari and S. An *et al.*, 2015. Integration of a MEMS-type vacuum pump with a MEMS-type Pirani pressure gauge. J. Vac. Sci. Technol. B Nanotechnol. Microelectron. Mater. Process. Meas. Phenom., 33: 03C103-03C103.

Joy, S. and J.K. Antony, 2015. Design and simulation of a micro hotplate using COMSOL multi-physics for MEMS based gas sensor. Proceedings of the 2015 IEEE 5th International Conference on Advances in Computing and Communications (ICACC'15), September 2-4, 2015, IEEE, Kochi,india, ISBN: 978-1-4673-6993-0, pp: 465-468.

Lasance, C.J.M., 2002. The thermal conductivity of air at reduced pressures and length scales. Electronic Cooling Inc., Santa Clara, California. https://www.electronics-cooling.com/2002/11/the-thermal-conductivity-of-air-at-reduced-pressures-and-length-scales/

Li, B. and H. Mou, 2016. Vacuum-sealed miniature modulated X-ray source and the influence factors of X-ray intensity. Chin. Opt. Lett., 14: 073401-073404.

Note, I.T.A., 2017. Bayard-alpert ionization gauges. Stanford Research Systems Inc., Sunnyvale, California.

Spallas, J., D. Meisburger and L. Muray, 2016. Ultralow voltage imaging using a miniature electron beam column. J. Vac. Sci. Technol. B Nanotechnol. Microelectron. Mater. Process. Meas. Phenom., 34: 06KB02-06KB02.